Highlights

-Quebracho tannin resin based foams prepared by combined mechanical and chemical expansion.

-Faster curing and expansion favoring its application as projected foams.

-Improved density and mechanical properties compared to foams only based in mechanical foaming.

PROJECTABLE TANNIN FOAMS BY MECHANICAL AND CHEMICAL EXPANSION

F.J. Santiago-Medina[a,*], A. Tenorio-Alfonso[b], C. Delgado-Sánchez[c], M.C. Basso[a], A. Pizzi[a,d,*], A. Celzard[c], V. Fierro[c], M.C. Sánchez[b], J.M. Franco[b]

[a] LERMAB, ENSTIB, University of Lorraine, 27 rue Philippe Séguin, BP 21042, 88051 Épinal cedex 9, France

[b] Pro2TecS-Chemical Product and Process Technology Research Centre, Department of Chemical Engineering, University of Huelva, Campus El Carmen, 21071 Huelva, Spain

[c] Institut Jean Lamour, UMR CNRS, University of Lorraine. ENSTIB, 27 rue Philippe Séguin, BP 21042, 88051 Epinal cedex 9, France

[d] Department of Physics, King Abdulaziz, Jeddah, Saudi Arabia

[*] Corresponding author at LERMAB, University of Lorraine, 27 rue Philippe Seguin, BP 21042, 88051 Epinal cedex 9, France. Fax: +33 3 29 29 61 38.
E-mail address: francisco-jose.santiago-medina@univ-lorraine.fr (F.J. Santiago-Medina).

Abstract

A new formulation of quebracho tannin-based resin has been used to prepare bio-based rigid foams. The proposed foams were blown by using the simultaneous combination of two expansion methods: by mechanical expansion as used for fire-fighting foams and by chemical expansion based on the release of water and other gases during the exothermal self-condensation of furfuryl alcohol. The combination of both methods allowed us to overcome certain limitations found in the preparation of foams exclusively based on mechanical expansion These were the resulting density (16% lower than that obtained by mechanical expansion) and the mechanical properties (compressive strength improved of about 11%). Resin chemorheology was characterized under stressed conditions using frequency and time sweeps as well as temperature ramps. The evolution of the linear viscoelastic functions during the reaction clearly showed the transition from viscous to strong gel-like behavior. The foaming and hardening processes were followed by the use of FOAMAT equipment and the resulting foams were characterized in terms of density (0.059-0.063 g/cm^3), mechanical properties (compressive strength of 0.090-0.144 MPa) and thermal conductivity (0.046-0.048 W m^{-1} K^{-1}).

Keywords

Tannin; Foams; Mechanical foaming; Chemical foaming; Rheology; Quebracho

1. Introduction

Condensed tannins are natural polyphenolic materials, which comprise a group of polyhydroxy-flavan-3-ol oligomers and polymers linked by carbon-carbon bonds between flavanol subunits (Schofield et al., 2001). They are used as one of the main components to prepare tannin-based rigid foams. These foams are a good substitute for commercial synthetic foams as they are environmentally friendly porous materials with excellent fire resistance properties and low thermal conductivity (Celzard et al., 2011; Tondi et al., 2008). They have also been used in other applications such as the preparation of lightweight sandwich panels (Tondi et al., 2016; Zhou et al., 2013). In addition, the improvement of hydrophobicity of tannin-based foams has been recently investigated (Delgado-Sánchez et al., 2016; Rangel et al., 2016).

Tannin-based foams can be prepared using different foaming systems. The most conventionally used foaming method is the physical one (Basso et al., 2015; Li et al., 2013). In the physical method, a solvent with low boiling point such as pentane or diethyl ether causes resin expansion due to solvent evaporation. The solvent boiling point is reached by the temperature increase caused by the exothermal self-condensation of furfuryl alcohol. Others foaming methods used in the preparation of tannin-based foams are chemical foaming (Basso et al., 2014), and mechanical foaming (Szczurek et al., 2014). The latter achieves the foaming of the tannin resin thanks to a surfactant and to the air introduced by energetic mechanical stirring. Finally, a last method of mechanical expansion based on firefighting foam systems has been recently developed (Santiago-Medina et al., 2018). All the foams obtained by these different methods tend to exhibit a common weakness**:** their mechanical properties are often inferior to those of the synthetic foams they are intended to replace. This is offset by the fact that they all employ sustainable, environmentally friendly additives and components.

Different rheological techniques have been successfully employed to mechanically characterize a large number of adhesives, coatings and related materials, such as polymeric adhesives (Mravljak and Šernek, 2011; Tenorio-Alfonso et al., 2017), polyurethane-based oleogels (Borrero-López et al., 2017; Gallego et al., 2013), bitumens (Carrera et al., 2014), tannin extracts (Garnier et al., 2001; Kim and Mainwaring, 1995), etc. These rheological characterizations give an insight on both, materials behavior under stressed conditions and their physical and mechanical stability by means of their viscous and viscoelastic responses, i.e. when viscous flow and oscillatory shear tests are applied to them. Moreover, oscillatory shear tests, frequency sweeps in particular, can be useful to obtain information about the molecular structure of the samples.

The decrease in thermal conductivity of foams, directly related to a decrease in their density, is one of the main challenges in the manufacture of tannin-based foams for insulation applications. Barriers to the decrease of the density of tannin foams prepared by mechanical foaming based on firefighting foams technology were found in previous works (Santiago-Medina et al., 2018). This research presents a new foam formulation where mechanical foaming, through the use of a foam concentrate, is combined with the chemical expansion provided by the self-condensation of furfuryl alcohol in acid medium to achieve a reduction in foam density. This approach generates a foam which could find application as a wall-projected foam, i.e. by directly spraying the foam on the wall. The resins used to prepare the foams have been characterized by rheological measurements (viscous flow, temperature ramp and frequency and time sweeps).

2. Material and methods

2.1. Materials

Sulphited quebracho (*Schinopsis lorentzii* and *Schinopsis balansae*) tannin extract, called Fintan T, was kindly supplied by SilvaChimica (S. Michele Mondovi, Italy). Furfuryl alcohol, Kolliphor ELP, glutarladehyde 50% water solution and glyoxal 40% water solution were provided by Sigma-Aldrich (France), and used as supplied. Phenolsulphonic acid 65% water solution was purchased at Capital Resin Corporation (Columbus, OH, USA). Ethoxylated oleyl amine, OAM-10, was supplied by Saibaba Surfactants Ltd (Gujarat, India) and the foaming agent used was SM2101, a proprietary product supplied by Condat (Chasse-sur-Rhone, France) mainly composed of alkyl glycols and modified fatty acid soaps.

2.2. Foam preparation

Foams formulations were prepared using the amounts of reagents listed in Table 1. The foams were made by mixing two components. The first component is formed by a homogeneous tannin resin (R1, which is composed by quebracho tannin, furfuryl alcohol, glutaraldheyde, glyoxal, and ethoxylated castor oil (Kolliphor ELP). Once the first component (R1) was prepared, the ethoxylated oleyl amine was added. The second component is a liquid mixture which contains the catalyst (acid or mixture of acids, as referred), the foam concentrate and the water. Using a special foaming blade stirrer as shown in Fig. 1, the second component was shaken at 2000 rpm during one minute to form a white liquid foam. The tannin resin was added immediately afterwards and the blend was stirred during 20s with the same stirrer. When the blending step was finished, a homogeneous brown liquid foam was obtained which was poured in a mould. This foam quickly expanded and hardened into a rigid foam.

The foam formulations described in Table 1 are: Standard, which was prepared using the above-mentioned method; WEA, the same that Standard foam but without using ethoxylated oleyl amine; S10, similar to Standard formulation but 10% of

116 phenolsulphonic acid was replaced by 10 % of sulfuric acid; and S20, where 20% of
117 phenolsulphonic acid was replaced by 20 % of sulfuric acid.

118 Table 1. Formulation components expressed in grams for each reactive.

Reactives (g)\Samples	Standard	WEA	S10	S20
Tannin (Quebracho)	10	10	10	10
Furfuryl alcohol	16	16	16	16
Glutaraldehyde (50 wt.%)	5	5	5	5
Glyoxal (40 wt.%)	15	15	15	15
Ethoxylated castor oil (Kolliphor ELP)	1	1	1	1
Ethoxylated oleyl amine (OAM-10)	1.5	-	1.5	1.5
SM2101 (Foam concentrate)	2.6	2.6	2.6	2.6
Water	3	3	3	3
Phenolsulphonic acid (65 wt.%)	17	17	15.3	13.6
Sulfuric acid	-	-	1.7	3.4

119

120 **2.3. Rheological characterization of the resin**

121 The tannin-based resin was rheologically characterized by using a controlled-stress
122 rheometer Haake MARS II (Thermo Fisher Scientific, Waltham, Massachusetts, USA).
123 Small-amplitude oscillatory shear (SAOS) tests were carried out within the linear
124 viscoelastic region (LVR) in a frequency range from 0.01-100 rad/s, at 25 and 100ºC,
125 using a cone-plate geometry (Ø 60 mm, 1º). The extension of the LVR was previously
126 evaluated by performing stress sweep tests at 1 Hz. In addition, viscous flow tests were
127 performed by imposing a stepped stress ramp in a stress range of 0.01 up to 100 Pa, at
128 25ºC. Curing process of the homogenous tannin resin was evaluated with the aid of time

sweep tests, using the same cone-plate geometry, at 25ºC and 1 Hz. Finally, natural resin was submitted to a heating rate of 2ºC/min, from 25-100ºC and at 1 Hz, by using a Physica MCR501 (Anton Paar GmbH, Ostfildern-Scharnhausen, Germany) equipped with a Peltier temperature controller and a cone-plate geometry (Ø 50 mm, 0.1 mm gap, 1º). All the rheological results were presented as the arithmetic average of at least two replicates.

2.4. Characterization of the rigid foams

2.4.1. Bulk density

The samples were cut in 30 × 30 × 15 mm^3 specimens and, afterwards, they were dried at ambient temperature during one week after preparation. Then, the bulk density, ρ_b, was calculated as the weight /volume ratio of each sample. Average value of 5 samples for each foam is shown.

2.4.2. Thermal conductivity

The transient plane source method (Hot Disk TPS 2500S) (Hot Disk AB, Gothemburg, Sweden) was used to carry out the thermal conductivity measurements. This method to calculate the thermal conductivity is based on a transiently heated plane sensor, which acts both as a heat source and as a dynamic temperature sensor, consisting of an electrically conducting pattern in the shape of a double spiral, which has been etched out of a thin nickel foil and sandwiched between two thin sheets of Kapton®. The plane sensor was fitted between two identical parallelepiped samples. The sensor used was C5501 with radius 6.403 mm. The conductivity was calculated by the Hot Disk 6.1 software.

2.4.3. Mechanical resistance

Compression tests were performed with an universal testing machine INSTRON 5944 (High Waycombe, UK) equipped with a 2 kN load cell. Samples of 30 × 30 × 15 mm^3 were compressed at 2 mm/min. All the curves presented the expected characteristics of cellular materials. The elastic modulus was defined as the slope of the first, linear region of the compression curve, and the compressive strength was defined as the height of the plateau region (Celzard et al., 2010). Three replicates were done for each foam.

2.4.4. Foaming capacity

The catalyzed resin was poured into the chamber of a FOAMAT 281 foaming measuring equipment (Format Messtechnik GmbH, Karlsruhe, Germany) and the different parameters were recorded during 1800s. This equipment measures and records simultaneously the expansion, hardening, and temperature and pressure variation during the foaming process. The chamber is composed of a cardboard cylinder set on the manometer sensor. The pressure generated by the expansion is measured by the force applied to the metal plate sensor. A K-type thermocouple is immersed into the mixture and measures the temperature variation. The CMD (Curing Monitor Device) sensor measures the foam's dielectric properties during the transition from liquid to solid state. It is a dielectric polarization sensor composed of two interdigitated electrodes disposed on a printed circuit in such a manner as to form a type of flat capacitor at the bottom of the foaming chamber. The foam height is constantly monitored by an ultrasound sensor according to the pulse-echo method. The software "Mousse", version 3.80, was used to collect and process the data.

3. Results and discussion

The apparent viscosity versus shear stress plot of the resin R1, at 25ºC, is shown in Fig. 2a. The different reagents of the resin R1 conferred to it an almost Newtonian behavior

with an average viscosity of 0.081 Pa·s. This makes the viscosity of the homogeneous tannin solution independent of the shear rate. This behavior is different from the one shown by the viscous flow of aqueous solutions of other tannin extracts, such as pine tannin extract, which exhibits a shear thinning behavior. This is due to the use of sodium sulphite for their extraction, that causes the cleavage of the interflavanoid bonds and the generation of lower molecular weight procyanidin-4-sulphonate derivates (Foo et al., 1983; Kim and Mainwaring, 1996; Pizzi, 1979).

Fig. 2b shows the frequency sweeps at 25ºC and 100ºC for the resin R1. In general, the viscous moduli (G'') is higher than the elastic one (G'), indicating a liquid-like behavior of the resin. However, at lower temperature (25ºC), the viscoelastic functions are more frequency-dependent, resulting in the typical evolution of Newtonian materials. Thus, for example, more frequency-dependent in the terminal region, with slopes of 2 and 1 for the G' and G'' vs. frequency plots, than at higher temperature (100ºC). This dependence with the frequency of both moduli at 25ºC indicates that the particles are sufficiently separate to avoid any interaction among them by Brownian motion or by repulsion or attraction potential (London or Van der Waals forces). Conversely, at higher temperature, it is normal that the frequency dependence decreases as a results of the greater number of interactions between particles. This is due to the increase in Brownian motions and even to some entanglements appearing. This leads to a decrease in the slope of both viscoelastic parameters vs. frequency plots, also associated to much more similar values. Therefore, a more solid-like behavior, not very different to the so called "critical gel" behavior (Lu et al., 2006), was found at 100ºC. This notwithstanding, at higher frequencies there is a crossover between both moduli (G'=G'') for both temperatures, after which G'>G''. This crossover at high frequencies just confirms that the resin behaves as a viscoelastic liquid, where no internal structure

or significant interaction among particles occurs. Thus, the resulting G' and G" vs. frequency curves are typical of non-structured polymer solutions and/or polymeric systems with a broad molecular weight distribution (Ferry, 1980; Goodyer, 2013; Mezger, 2002), as it is the case for the distribution of the different chain sizes of quebracho tannin oligomers (Pasch et al., 2001; Radebe et al., 2013; Vivas et al., 2004).

The evolution of SAOS functions for resin R1 obtained under curing conditions is shown in Fig. 3. The temperature ramp, from 25ºC to 100ºC (at 2ºC/min and 1 Hz) displays two well-defined regions:

-The first region, from 25ºC to 75ºC, is characterized by tan $\delta >> 1$, which indicates a clear fluid-like behavior. The increase in temperature involves a slight decrease in G' and G'', tipically due to thermal agitation. This trend changes due to the increase in particles interaction, thus, rising the values of both moduli, G' and G'', and also decreasing the values of tan δ respectively (Cordobés et al., 2004).

-In the second region from 75ºC to 100ºC, tan δ is still decreasing until an asymptotic value close to 1, and the slopes of both moduli also tend to a plateau. In this region, the sol-gel transition is almost reached (Sánchez and Burgos, 1997) despite that there is not a clear crossover between both moduli curves.

Fig. 4 shows the evolution of the SAOS functions with time, at 25ºC, once the resin R1 has been mixed with the ethoxylated oleyl amine and the second component (without foaming concentrate). This test allows to follow the reaction that occurs in the resin during hardening. Throughout the whole experimental time range considered, G' values remain higher than G" ones (tan $\delta < 1$) that clearly indicates the solid-like behavior of the mixture. This result was expected, since the second component contains the phenolsulphonic acid (catalyst) which creates the acid conditions, triggering the self-

condensation reaction of furfuryl alcohol. Furfuryl alcohol self-crondenses and crosslinks with the others components of the resin. This also promotes the reaction of the other components, due to the increase in temperature caused by the heat released during its self-condensation reaction. These reactions lead to the formation of a highly structured network that causes the transition from a liquid resin to a solid-like material which becomes progressively harder as crosslinking proceeds further. The hardening is enough advanced developed from 320-350 s of reaction when disturbances in the viscoelastic functions in the time sweep and, afterwards, developing a tendency to reach a plateau is observed.

Fig. 5 shows the evolution of different parameters of the foam such as the temperature, the dielectric polarization and the foam height as a function of time, during the foaming and hardening process. The main difference between this new kind of tannin foam and previously reported tannin foams is the use of mechanical foaming in a combination with a well-controlled chemical foaming process based on the self-condensation of furfuryl alcohol. The mechanical foaming was achieved by the use of a special mechanical stirrer (Fig. 1) and a foam concentrate to obtain a stable liquid foam. The reaction of self-condensation in acid medium caused an additional expansion of the liquid foam due to the release of water vapour and of the other gases generated. This is also a consequence of the heat released during the condensation reaction. The temperature increment within the foam induces crosslinking reactions among the components of the resin, hardening the tannin cellular structure formed during mechanical expansion. The temperature (Fig. 5a) displays the characteristic progression which has already been reported in the literature (Basso et al., 2013; Lacoste et al., 2015). This is characterized by a quick increase in temperature until a maximum that matches with the first and highest maximum in dielectric polarization. The simultaneity

of these two peaks is a good indication that the formulation is well-balanced and that the risk of shrinkage is almost avoided. This is due to the fact that hardening began just when the expansion had finished, providing rigidity to the tannin structure. The absence of shrinkage can be observed in Fig. 5c, where the maximum height reached after the expansion was kept constant during the rest of the measurements. This is less evident for the samples without ethoxylated oleyl amine (WEA) where a slight shrinkage is observed. That lack of shrinkage is also probably due to the presence of oleyl chains of the surfactant among the other components of the mixture. The oleyl chains help to maintain the structure in place while the structure becomes hard enough. It should also be noted in Fig. 5c that there is a first initial height, more visible for Standard and WEA, due to the expansion of the resin after the initial mechanical expansion.

Conversely, Fig. 5b shows the evolution of the dielectric polarization. Two well-defined peaks are observed in the spectrum, which may be associated to two different groups of reactions. The first one mainly belongs to the self-condensation reaction of furfuryl alcohol in presence of acid. The second peak, much broader than the first one, belongs to the crosslinking reaction of glutaraldheyde and glyoxal with the tannin and the other reactive compounds to form a hard network. These results are in agreement with the destabilization observed in the time sweep diagram (Fig. 4), occurring around 330 s, just after this second broad peak in the dielectric polarization curve. This indicates that the structure presents a high level of hardness and also that the foam concentrate does not have a direct influence on the resin hardening process. Although it is not a scientific test, around 8-10 minutes after the expansion, the foam is hard enough and can be cut with a knife without risk to damage the cellular network.

Table 2. Results of the characterization of the foams.

	Standard	WEA	S10	S20
Bulk density (g/cm^3)	0.059	0.063	0.061	0.062
Thermal conductivity (W m^{-1} K^{-1})	0.046	0.048	0.047	0.047
Elastic modulus (MPa)	4.92	3.54	2.71	1.76
Compressive strength (MPa)	0.144	0.108	0.106	0.090

The results of the tannin foams characterization are gathered in Table 2. The use of the combination of mechanical and chemical expansion in the preparation of foams allows to obtain lower density foams than those obtained by means of mechanical expansion only (density around 0.071 g/cm^3) (Santiago-Medina et al., 2018). In addition, the low densities obtained are comparable with those of other tannin foams which include some foaming agent, as pentane or diethyl ether (Celzard et al., 2010; Lacoste et al., 2013b; Meikleham and Pizzi, 1994; Tondi et al., 2009). The therrmal conductivity of the prepared foams depends on their density due to their open-cell structure, as for other tannin-furanic foams described previously in literature. The thermal conductivity values of these foams are comparable with those already reported in the literature for other tannin foams already published (Basso et al., 2014; Basso et al., 2015; Li et al., 2012). Overall, all the results are within the range of the most common insulation materials (0.020-0.055 W m^{-1} K^{-1}) according to the Federation of European rigid Polyurethane foam associations, and therefore they can be considered as good insulators (FERPFA, 2006).

Foams usually exhibit a compression stress-strain curve corresponding to three different behaviors of the material. There is an initial linear step with the elastic behavior of the foam controlled by cell wall bending. This region is followed by a plateau due to the collapse of the cells, and finally a third region called densification, which occurs when all the cells are collapsed. Fig.6 shows the compression curves of the foams

studied—one of the repetitions for each foam— of the foams studied, which perfectly display the three regions mentioned above. The main mechanical parameters obtained are gathered in Table 2. The results of the compression test of these mixed foams are much better than those prepared only by mechanical expansion (Santiago-Medina et al., 2018). They also present better or comparable mechanical properties of other tannin foams with similar densities, which used some additives to improve such properties (Basso et al., 2015; Lacoste et al., 2013a; Li et al., 2012). Finally, the compressive strength values obtained are suitable to foams with an application as insulating materials (FERPFA, 2006). However, the role of sulfuric acid in such foams should be emphasized. The substitution of sulphuric acid by a part of phenolsulphonic acid reduces the induction time considerably (time at which the temperature starts to increase, producing the beginning of the expansion). Thus, 10% (S10) and 20% (S20) of substitution decreases the induction time by 15 and 30s respectively. However, the mechanical properties are adversely affected. Sulfuric acid is well-known for having a corrosive effect on organic matter, resulting in a loss of mechanical properties. Even with these degradation in the properties, the material is still suitable for application. Therefore, either a balance between acceleration and reduction of mechanical properties, or the replacement of sulfuric acid by an acid stronger than phenolsulfonic acid, but less corrosive than sulfuric acid, can be envisaged.

4. **Conclusions**

Quebracho tannin-based rigid foams were prepared using a novel methodology which combines the mechanical expansion based on the fire-fighting foams technology with the chemical expansion of the resin to achieve the foaming. This procedure leads to a decrease of foam density in relation to foams prepared previously exclusively by mechanical methods. This is beneficial. In addition, these new foam formulations show

mechanical and thermal properties within the frameworks established by the Federation of European rigid Polyurethane foam associations, and, therefore, they can be considered as good insulators.

The rheological response of tannin resins follows a Newtonian behavior under stressed conditions, whereas the evolution of the linear viscoelastic functions during the reaction shows the transition from viscous to strong gel-like behavior.

Conversely, the foaming and curing times have also been decreased in relation to the traditional mechanical methods. The latter can be controlled by the regulation of the dose of acids, letting the expansion and the hardening of the foam to occur more rapidly. This could reduce the time that the liquid foam stays on the wall before hardening, as in the potential application as a wall-projected foam.

Acknowledgements

The authors acknowledge the funding from the BRIIO project, financed by the conventions of the French state (FUI) Nr. 1410042V and Nr. 1410043V through Bpifrance financement, and TEP-1499 project, funded by the Andalusian Regional Government, respectively. One of the authors (Adrián Tenorio) also acknowledges award of a PhD grant from Spain's Ministry of Education (FPU13/01114).

References

Basso, M.C., Giovando, S., Pizzi, A., Celzard, A., Fierro, V., 2013. Tannin/furanic foams without blowing agents and formaldehyde. Ind. Crops Prod. 49, 17–22. https://doi.org/10.1016/j.indcrop.2013.04.043

Basso, M.C., Lagel, M.C., Pizzi, A., Celzard, A., Abdalla, S., 2015. First Tools for Tannin-Furanic Foams Design. BioResources 10, 5233–5241. https://doi.org/10.157376/biores.10.3.5233-5241

Basso, M.C., Pizzi, A., Lacoste, C., Delmotte, L., Al-Marzouki, F., Abdalla, S., Celzard, A., 2014. MALDI-TOF and 13C NMR Analysis of Tannin–Furanic–Polyurethane Foams Adapted

for Industrial Continuous Lines Application. Polymers 6, 2985–3004. https://doi.org/10.3390/polym6122985
Borrero-López, A.M., Santiago-Medina, F.J., Valencia, C., Eugenio, M.E., Martin-Sampedro, R., Franco, J.M., 2017. Valorization of Kraft Lignin as Thickener in Castor Oil for Lubricant Applications. J. Renew. Mater. https://doi.org/10.7569/JRM.2017.634160
Carrera, V., Cuadri, A.A., García-Morales, M., Partal, P., 2014. Influence of the prepolymer molecular weight and free isocyanate content on the rheology of polyurethane modified bitumens. Eur. Polym. J. 57, 151–159. https://doi.org/10.1016/j.eurpolymj.2014.05.013
Celzard, A., Fierro, V., Amaral-Labat, G., Pizzi, A., Torero, J., 2011. Flammability assessment of tannin-based cellular materials. Polym. Degrad. Stab. 96, 477–482. https://doi.org/10.1016/j.polymdegradstab.2011.01.014
Celzard, A., Zhao, W., Pizzi, A., Fierro, V., 2010. Mechanical properties of tannin-based rigid foams undergoing compression. Mater. Sci. Eng. A 527, 4438–4446. https://doi.org/10.1016/j.msea.2010.03.091
Cordobés, F., Partal, P., Guerrero, A., 2004. Rheology and microstructure of heat-induced egg yolk gels. Rheol. Acta 43, 184–195. https://doi.org/10.1007/s00397-003-0338-3
Delgado-Sánchez, C., Letellier, M., Fierro, V., Chapuis, H., Gérardin, C., Pizzi, A., Celzard, A., 2016. Hydrophobisation of tannin-based foams by covalent grafting of silanes. Ind. Crops Prod. 92, 116–126. https://doi.org/10.1016/j.indcrop.2016.08.002
FERPFA, 2006. Thermal insulation materials made of rigid polyurethane foam (PUR/PIR) (Report No. 1). Federation of European rigid Polyurethane foam associations, Bruxelles, Belgium.
Ferry, J.D., 1980. Viscoelastic properties of polymers, 3d ed. ed. Wiley, New York.
Foo, L.Y., McGraw, G.W., Hemingway, R.W., 1983. Condensed tannins: preferential substitution at the interflavanoid bond by sulphite ion. J. Chem. Soc. Chem. Commun. 672. https://doi.org/10.1039/c39830000672
Gallego, R., Arteaga, J.F., Valencia, C., Franco, J.M., 2013. Rheology and thermal degradation of isocyanate-functionalized methyl cellulose-based oleogels. Carbohydr. Polym. 98, 152–160. https://doi.org/10.1016/j.carbpol.2013.04.104
Garnier, S., Pizzi, A., Vorster, O.C., Halasz, L., 2001. Comparative rheological characteristics of industrial polyflavonoid tannin extracts. J. Appl. Polym. Sci. 81, 1634–1642. https://doi.org/10.1002/app.1594
Goodyer, S., 2013. Measuring polymers using a rotational rheometer in oscillatory mode.
Kim, S., Mainwaring, D.E., 1996. Influence of Viscosity Modifying Agents on *Pinus radiata* Extract. Holzforschung 50, 42–48. https://doi.org/10.1515/hfsg.1996.50.1.42
Kim, S., Mainwaring, D.E., 1995. Rheological characteristics of proanthocyanidin polymers from Pinus radiata. II. Viscoelastic properties of sequential alkaline extracts based on phenolic acid fraction. J. Appl. Polym. Sci. 56, 915–924. https://doi.org/10.1002/app.1995.070560805
Lacoste, C., Basso, M.C., Pizzi, A., Laborie, M.-P., Celzard, A., Fierro, V., 2013a. Pine tannin-based rigid foams: Mechanical and thermal properties. Ind. Crops Prod. 43, 245–250. https://doi.org/10.1016/j.indcrop.2012.07.039
Lacoste, C., Basso, M.C., Pizzi, A., Laborie, M.-P., Garcia, D., Celzard, A., 2013b. Bioresourced pine tannin/furanic foams with glyoxal and glutaraldehyde. Ind. Crops Prod. 45, 401–405. https://doi.org/10.1016/j.indcrop.2012.12.032
Lacoste, C., Čop, M., Kemppainen, K., Giovando, S., Pizzi, A., Laborie, M.P., Sernek, M., Celzard, A., 2015. Biobased foams from condensed tannin extracts from Norway spruce (Picea abies) bark. Ind. Crops Prod. 73, 144–153. https://doi.org/10.1016/j.indcrop.2015.03.089

399 Li, X., Essawy, H.A., Pizzi, A., Delmotte, L., Rode, K., Le Nouen, D., Fierro, V., Celzard, A., 2012.
400 Modification of tannin based rigid foams using oligomers of a hyperbranched
401 poly(amine-ester). J. Polym. Res. 19. https://doi.org/10.1007/s10965-012-0021-4
402 Li, X., Pizzi, A., Lacoste, C., Fierro, V., Celzard, A., 2013. Physical Properties of Tannin/Furanic
403 Resin Foamed With Different Blowing Agents. Bioresources 8, 743–752.
404 Lu, L., Liu, X., Tong, Z., 2006. Critical exponents for sol–gel transition in aqueous alginate
405 solutions induced by cupric cations. Carbohydr. Polym. 65, 544–551.
406 https://doi.org/10.1016/j.carbpol.2006.02.010
407 Meikleham, N.E., Pizzi, A., 1994. Acid- and alkali-catalyzed tannin-based rigid foams. J. Appl.
408 Polym. Sci. 53, 1547–1556. https://doi.org/10.1002/app.1994.070531117
409 Mezger, T.G., 2002. The rheology handbook: for users of rotational and oscillation rheometers,
410 Coatings compendia. Vincentz, Hannover.
411 Mravljak, M., Šernek, M., 2011. The Influence of Curing Temperature on Rheological Properties
412 of Epoxy Adhesives. Drv. Ind. 19–25. https://doi.org/10.5552/drind.2011.1042
413 Pasch, H., Pizzi, A., Rode, K., 2001. MALDI–TOF mass spectrometry of polyflavonoid tannins.
414 Polymer 42, 7531–7539. https://doi.org/10.1016/S0032-3861(01)00216-6
415 Pizzi, A., 1979. Sulphited tannins for exterior wood adhesives. Colloid Polym. Sci. 257, 37–40.
416 https://doi.org/10.1007/BF01539014
417 Radebe, N., Rode, K., Pizzi, A., Pasch, H., 2013. Microstructure elucidation of polyflavonoid
418 tannins by MALDI-TOF-CID. J. Appl. Polym. Sci. 127, 1937–1950.
419 https://doi.org/10.1002/app.37568
420 Rangel, G., Chapuis, H., Basso, M.-C., Pizzi, A., Delgado-Sanchez, C., Fierro, V., Celzard, A.,
421 Gerardin-Charbonnier, C., 2016. Improving Water Repellence and Friability of Tannin-
422 Furanic Foams by Oil-Grafted Flavonoid Tannins. BioResources 11.
423 https://doi.org/10.15376/biores.11.3.7754-7768
424 Sánchez, A.C., Burgos, J., 1997. Gelation of sunflower globulin hydrolysates: rheological and
425 calorimetric studies. J. Agric. Food Chem. 45, 2407–2412.
426 https://doi.org/10.1021/jf960867+
427 Santiago-Medina, F.J., Delgado-Sánchez, C., Basso, M.C., Pizzi, A., Fierro, V., Celzard, A., 2018.
428 Mechanically blown wall-projected tannin-based foams. Ind. Crops Prod. 113, 316–
429 323. https://doi.org/10.1016/j.indcrop.2018.01.049
430 Schofield, P., Mbugua, D.M., Pell, A.N., 2001. Analysis of condensed tannins: a review. Anim.
431 Feed Sci. Technol., Tannins:Analysis and Biological Effects in Ruminant Feeds 91, 21–
432 40. https://doi.org/10.1016/S0377-8401(01)00228-0
433 Szczurek, A., Fierro, V., Pizzi, A., Stauber, M., Celzard, A., 2014. A new method for preparing
434 tannin-based foams. Ind. Crops Prod. 54, 40–53.
435 https://doi.org/10.1016/j.indcrop.2014.01.012
436 Tenorio-Alfonso, A., Sánchez, M.C., Franco, J.M., 2017. Preparation, Characterization and
437 Mechanical Properties of Bio-Based Polyurethane Adhesives from Isocyanate-
438 Functionalized Cellulose Acetate and Castor Oil for Bonding Wood. Polymers 9, 132.
439 https://doi.org/10.3390/polym9040132
440 Tondi, G., Link, M., Kolbitsch, C., Lesacher, R., Petutschnigg, A., 2016. Pilot plant up-scaling of
441 tannin foams. Ind. Crops Prod. 79, 211–218.
442 https://doi.org/10.1016/j.indcrop.2015.11.013
443 Tondi, G., Pizzi, A., Olives, R., 2008. Natural tannin-based rigid foams as insulation for doors
444 and wall panles. Maderas Cienc. Tecnol. 10, 219–227. https://doi.org/10.4067/S0718-
445 221X2008000300005
446 Tondi, G., Zhao, W., Pizzi, A., Du, G., Fierro, V., Celzard, A., 2009. Tannin-based rigid foams: A
447 survey of chemical and physical properties. Bioresour. Technol. 100, 5162–5169.
448 https://doi.org/10.1016/j.biortech.2009.05.055
449 Vivas, N., Nonier, M.-F., de Gaulejac, N.V., Absalon, C., Bertrand, A., Mirabel, M., 2004.
450 Differentiation of proanthocyanidin tannins from seeds, skins and stems of grapes

(Vitis vinifera) and heartwood of Quebracho (Schinopsis balansae) by matrix-assisted laser desorption/ionization time-of-flight mass spectrometry and thioacidolysis/liquid chromatography/electrospray ionization mass spectrometry. Anal. Chim. Acta 513, 247–256. https://doi.org/10.1016/j.aca.2003.11.085

Zhou, X., Pizzi, A., Sauget, A., Nicollin, A., Li, X., Celzard, A., Rode, K., Pasch, H., 2013. Lightweight tannin foam/composites sandwich panels and the coldset tannin adhesive to assemble them. Ind. Crops Prod. 43, 255–260. https://doi.org/10.1016/j.indcrop.2012.07.020

Figure legend

Fig. 1. Foaming blade

Fig. 2. Viscous flow at 25ºC (a) and frequency sweeps at 25ºC and 100ºC (b) for the resin R1.

Fig. 3. Temperature ramp for the resin R1.

Fig. 4. Time sweep of the mixture resulting from resin R1, the ethoxylated oleyl amine and the second component.

Fig. 5. Foamat results for the four samples: (a) temperature, (b) dielectric polarization, and (c) height, as a function of time.

Fig. 6. Stress-strain curves for a sample of each of the foams presented in Table 2 submitted to compression.

Figure 1

Figure 2

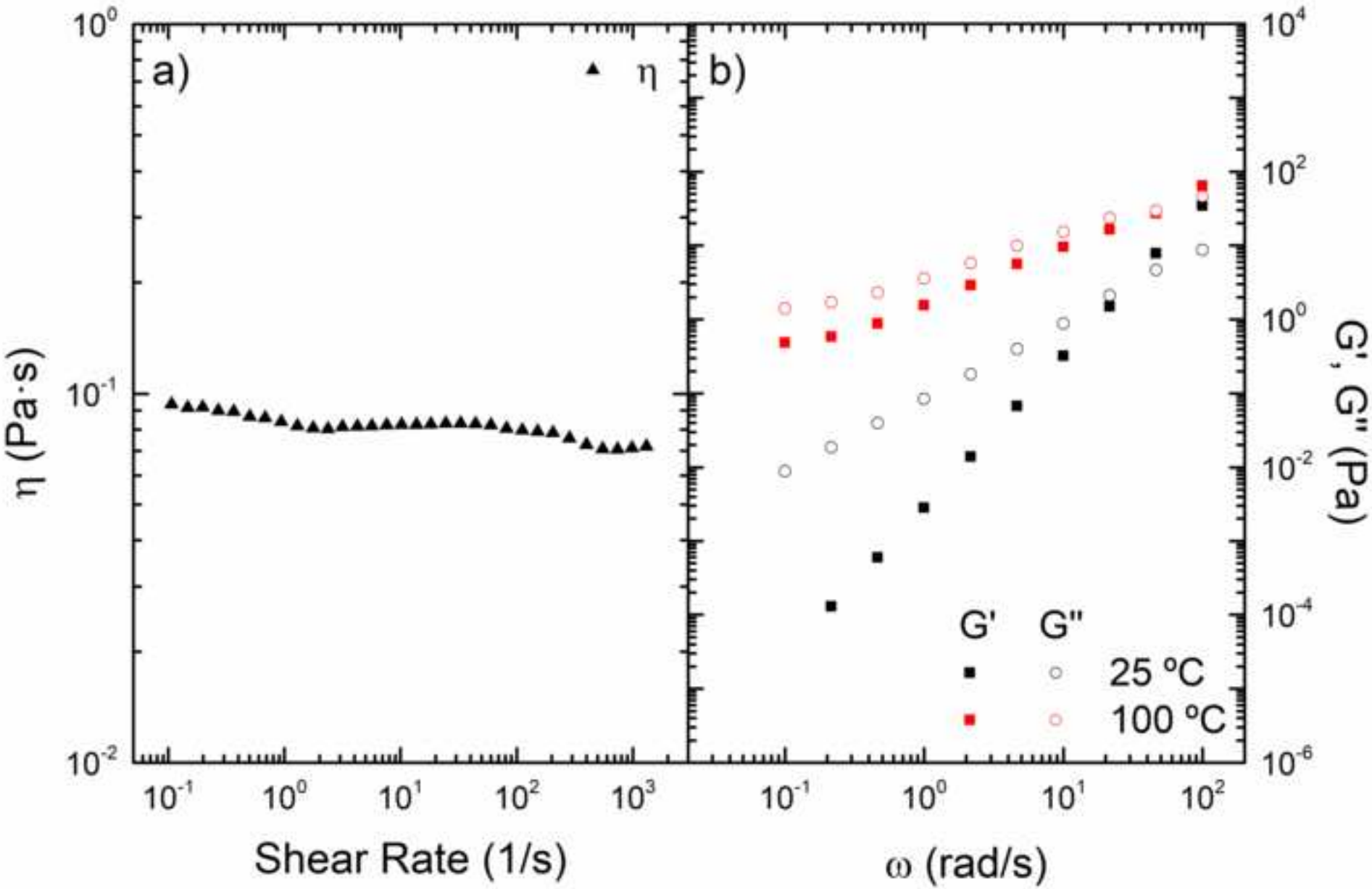
a)
η
b)
η (Pa·s)
Shear Rate (1/s)
ω (rad/s)
G', G'' (Pa)
G'
G''
25 °C
100 °C
10^0
10^-1
10^-2
10^1
10^2
10^3
10^4
10^-4
10^-6

Figure 3

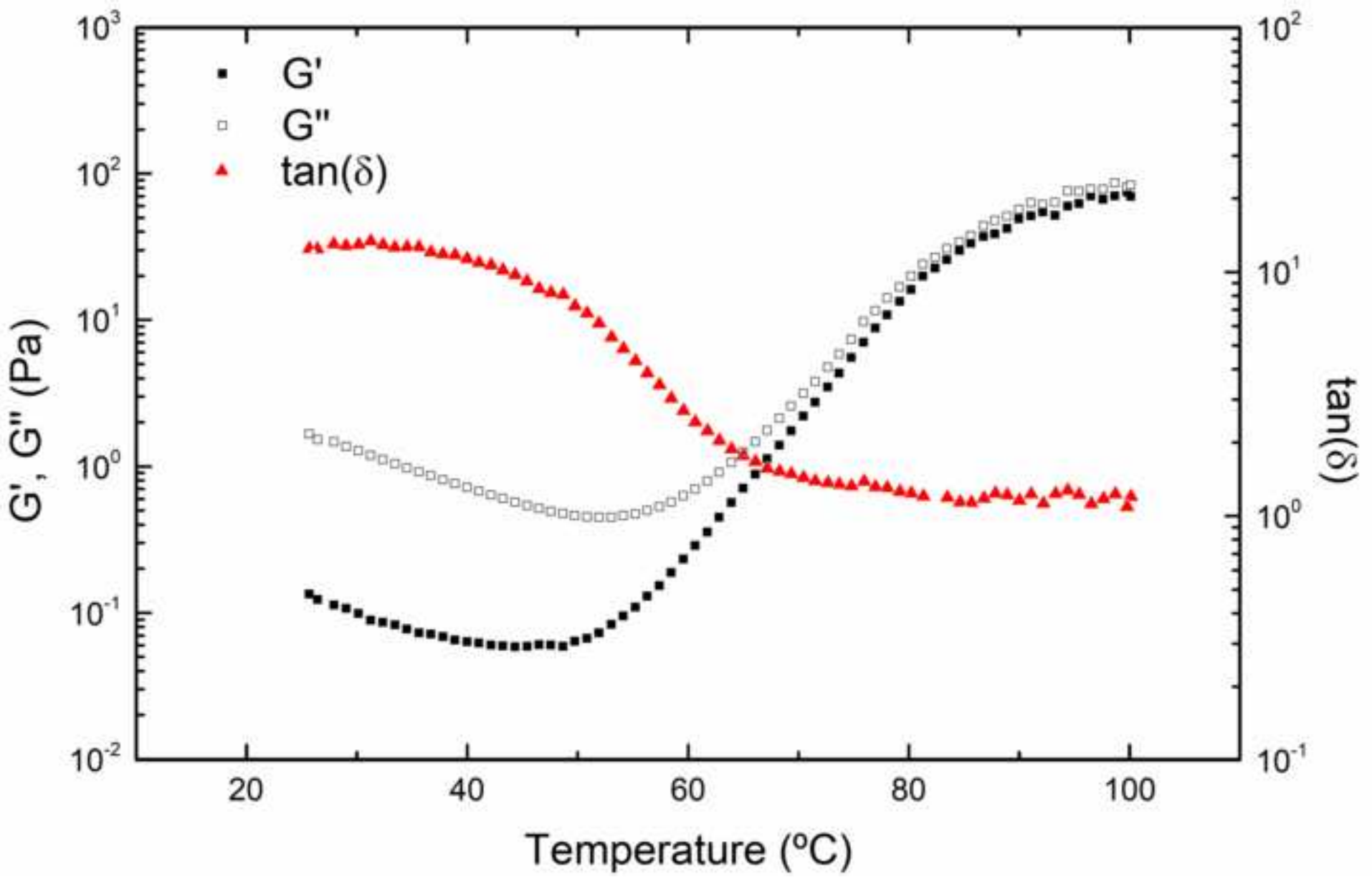
G'
G''
tan(δ)
G', G'' (Pa)
tan(δ)
Temperature (ºC)
10^3
10^2
10^1
10^0
10^-1
10^-2
10^2
10^1
10^0
10^-1
20
40
60
80
100

Figure 4

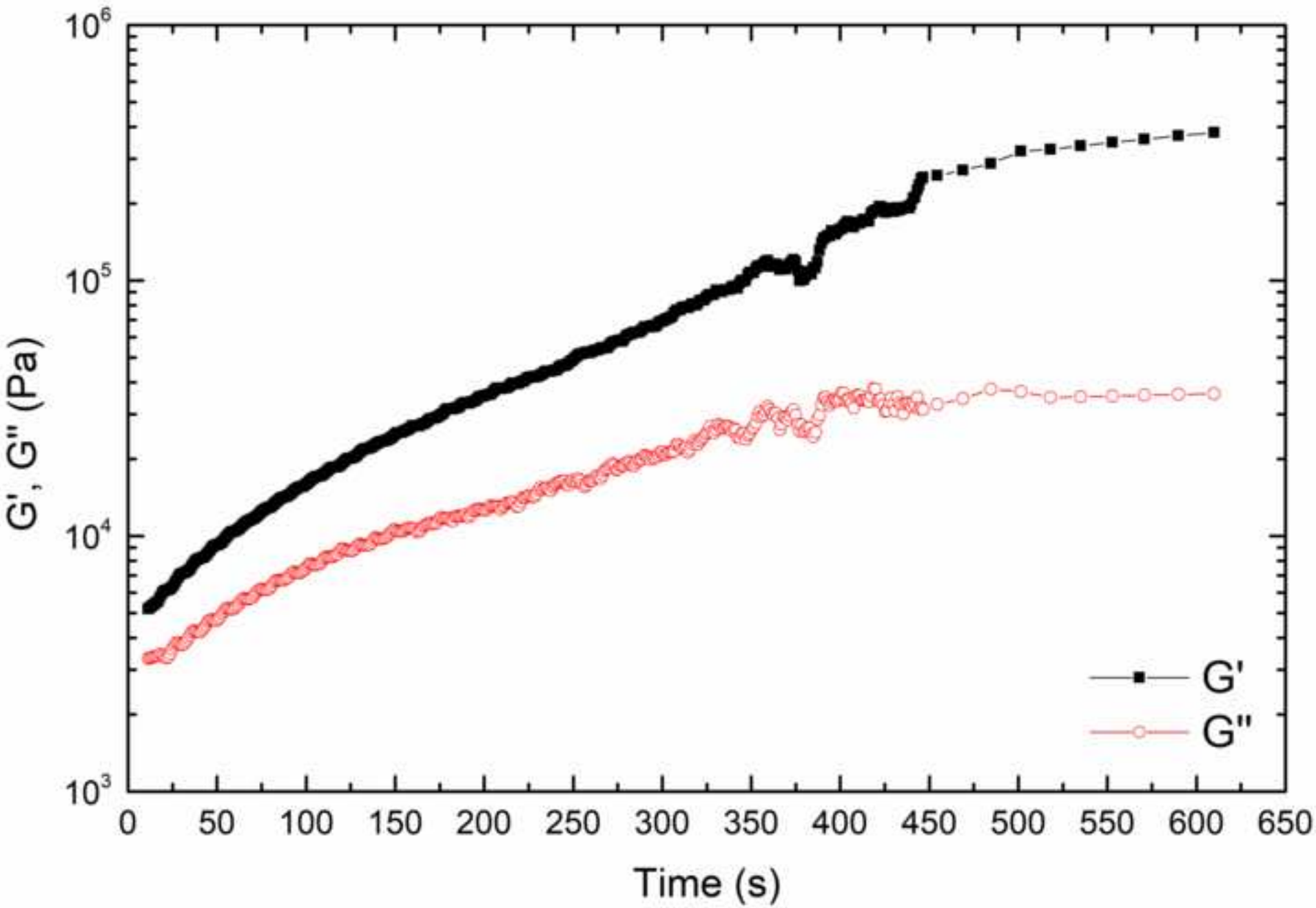
10^6
10^5
10^4
10^3
G', G'' (Pa)
0
50
100
150
200
250
300
350
400
450
500
550
600
650
Time (s)
G'
G''

Figure 5

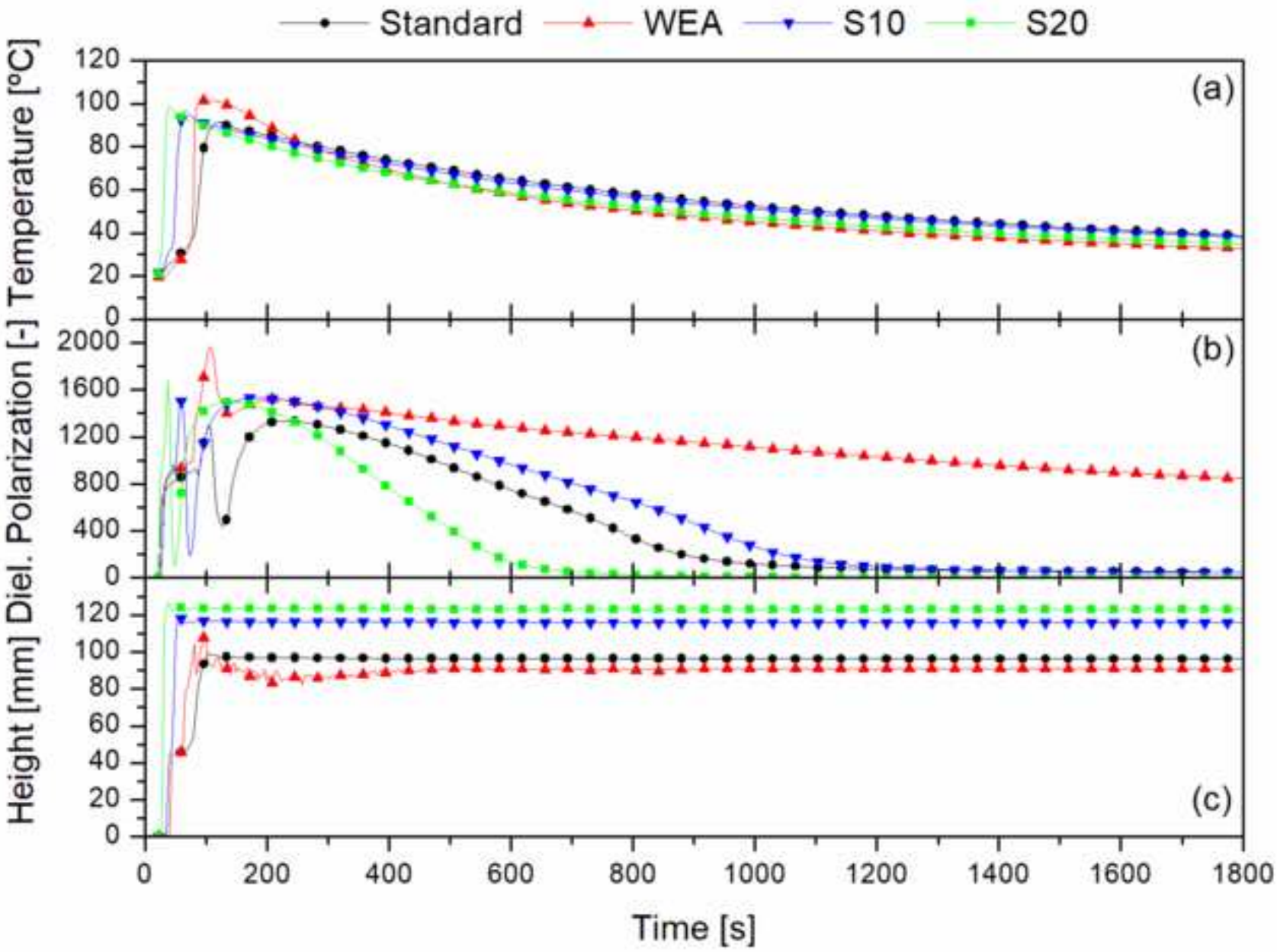
Standard
WEA
S10
S20
Height [mm] Diel. Polarization [-] Temperature [°C]
(a)
(b)
(c)
Time [s]
0
200
400
600
800
1000
1200
1400
1600
1800

Figure 6

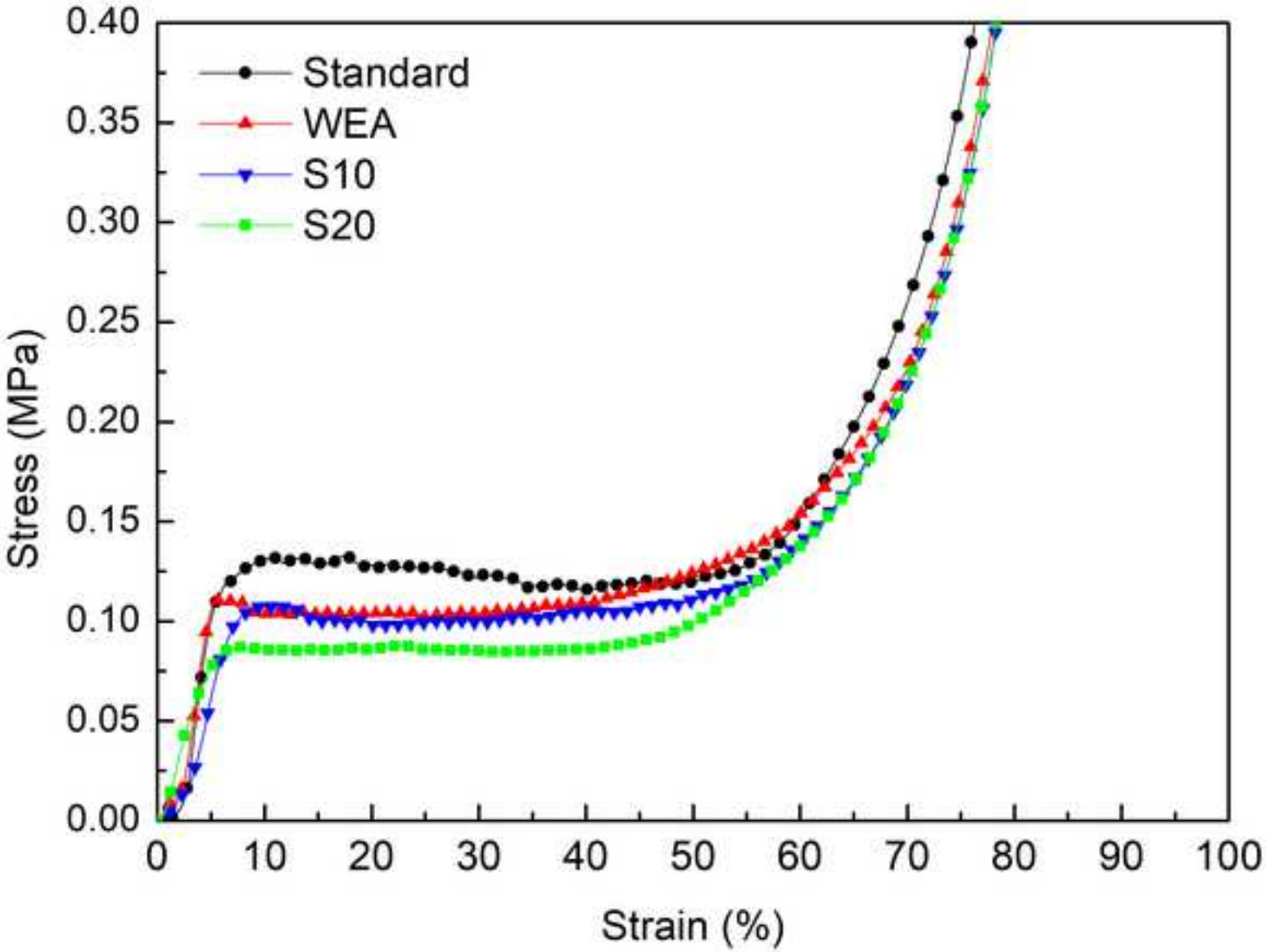
Standard
WEA
S10
S20
Stress (MPa)
Strain (%)
0.00
0.05
0.10
0.15
0.20
0.25
0.30
0.35
0.40
0
10
20
30
40
50
60
70
80
90
100